

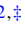





## Fine structure of the doublet $P$ levels of boron

Saeed Nasiri <sup>1,\*</sup> Dmitry Tumakov <sup>1,†</sup> Monika Stanke <sup>2,‡</sup> Andrzej Kędziorowski <sup>2,§</sup>  
Ludwik Adamowicz <sup>3,4,||</sup> and Sergiy Bubin <sup>1,¶</sup>

<sup>1</sup>*Department of Physics, Nazarbayev University, Astana 010000, Kazakhstan*

<sup>2</sup>*Institute of Physics, Faculty of Physics, Astronomy, and Informatics,  
Nicolaus Copernicus University, ul. Grudziądzka 5, Toruń PL 87-100, Poland*

<sup>3</sup>*Department of Chemistry and Biochemistry, University of Arizona, Tucson, Arizona 85721, USA*

<sup>4</sup>*Department of Physics, University of Arizona, Tucson, Arizona 85721, USA*



(Received 10 May 2024; accepted 7 August 2024; published 2 December 2024)

We report high-accuracy calculations of the ground and the lowest eight excited  ${}^2P^o$  states of the two stable isotopes of the boron atom,  ${}^{10}\text{B}$  and  ${}^{11}\text{B}$ , as well as of the boron atom with an infinite nuclear mass  ${}^\infty\text{B}$ . The nonrelativistic wave function of each of the states is generated in an independent variational calculation by expanding it in terms of a large number, 12 000–17 000, of all-electron explicitly correlated Gaussian (ECG) functions whose nonlinear parameters are extensively optimized with a procedure that employs analytic energy gradient determined with respect to these parameters. These highly accurate wave functions are used to compute the fine-structure splittings using the first order of the perturbation theory ( $\sim\alpha^2$ ), where  $\alpha$  is the fine-structure constant, which are then corrected for the electron magnetic moment anomaly ( $\sim\alpha^3$ ). As the nonrelativistic Hamiltonian explicitly depends on the mass of the nucleus, the recoil corrections up to the order of  $\alpha^2$  are automatically accounted for in the fine-structure calculations. Furthermore, the off-diagonal corrections to the fine structure ( $\sim\alpha^4$ ) are estimated using the multireference methods based on one-electron Gaussian orbitals. The results obtained in this paper are considerably more accurate than those available in the literature. Moreover, we report accurate splittings for a number of excited  ${}^2P^o$  states, for which there have been no reliable experimental or theoretical data at all. The calculated values presented in this paper may serve as a valuable guide for future experimental measurements of the fine structure of the boron atom. As the fine structure of an atom provides a spectral signature that can facilitate atom's detection, our data can also aid the search for trace amounts of boron in the interstellar medium.

DOI: [10.1103/PhysRevResearch.6.043225](https://doi.org/10.1103/PhysRevResearch.6.043225)

### I. INTRODUCTION

In the cosmological hierarchy of elemental abundances, boron does not approach the prevalence of primordial hydrogen or helium, nor does it rival the quantities of heavier nucleosynthetic products such as carbon. Indeed, boron's presence in the universe is scarce [1]. However, boron occupies a unique position within cosmic studies, being synthesized in minimal amounts during the terminal nuclear fusion processes of stars and via the cosmic ray-mediated fragmentation of more massive elements present in the interstellar medium [2]. The elemental scarcity of boron,

juxtaposed with its unique formation pathways, renders it a probe of exceptional value in the examination of astrophysical phenomena, providing insights into the underpinnings of cosmic ray interactions and the nucleosynthetic history of the universe [3,4]. Furthermore, the previous studies showed that the fine-structure transitions can be used to estimate the density of the absorbing medium or the ambient intensity of a strong photon flux and relative abundance of  ${}^{10}\text{B}$  and  ${}^{11}\text{B}$  isotopes [5–8].

Despite the importance of the spectral properties of the boron atom, very few *accurate* experimental and theoretical studies of these properties have been reported in the literature. The most accurate experimental measurements are mainly available for gases composed of highly volatile elements, including boron. In general, creating gaseous samples with a sufficient optical density can be quite challenging. For instance, the available fine-structure splitting measurements of boron show relatively poor agreement with each other [9,10]. On the theoretical side, because of the complexity of the electronic structure of the boron atom, even most accurate electronic structure methods such as coupled-cluster (CC) [11] or multiconfiguration Hartree–Fock (MCHF) [12] have not been capable to provide a reasonably accurate estimation of the fine-structure splittings of the boron atom. It is

\* Contact author: saeed.nasiri@nu.edu.kz

† Contact author: dm.tumakov@gmail.com

‡ Contact author: monika@fizyka.umk.pl

§ Contact author: andrzej.kedziorowski@fizyka.umk.pl

|| Contact author: ludwik@arizona.edu

¶ Contact author: sergiy.bubin@nu.edu.kz

Published by the American Physical Society under the terms of the [Creative Commons Attribution 4.0 International](https://creativecommons.org/licenses/by/4.0/) license. Further distribution of this work must maintain attribution to the author(s) and the published article's title, journal citation, and DOI.

also worth mentioning that in the aforementioned theoretical studies, the finite nuclear mass effect was not considered in the calculations and the reported values were obtained for the boron atom with an infinite nuclear mass ( $^{\infty}\text{B}$ ). In other words, the calculations were performed by assuming the Born-Oppenheimer (BO) approximation. The most accurate value for the fine-structure splitting in the ground state of the  $^{11}\text{B}$  isotope was computed in Ref. [13] using all electron explicitly correlated Gaussian (ECG) basis functions. Their values are in good agreement with the data available in the NIST ASD database [14]. However, they did not provide any values for the  $^{10}\text{B}$  isotope, which is as important as the  $^{11}\text{B}$  isotope in astronomical studies. The value of the fine-structure splitting of the ground state [ $1s^2 2s^2 2p(^2P)$ ] of the boron atom presented in this paper is in full agreement with the value obtained in Ref. [13] and improves it by reducing the numerical uncertainty. However, in addition to the ground-state calculations for  $^{10}\text{B}$  and  $^{11}\text{B}$ , we also carry out calculations for the lowest eight excited  $^2P$  states.

We should mention that spectral properties of the boron atom were a subject of our previous studies that employed all-electron ECG basis functions and the variational approach [15–17]. The variational calculations were used to optimize the ECG nonlinear parameters with a procedure that employs the analytical derivatives of the nonrelativistic non-Born-Oppenheimer (non-BO) energy of the atom determined with respect to the nonlinear parameters. The use of the analytic energy gradient greatly expedited the optimization process and allowed for achieving very high accuracy in the calculations. The purpose of the present paper is to use a similar approach to enhance and refine the currently available computational data concerning the fine-structure splittings of both stable isotopes of boron ( $^{10}\text{B}$  and  $^{11}\text{B}$ ), as well as of the boron atom with an infinite nuclear mass ( $^{\infty}\text{B}$ ). The efficacy and precision of the method for the fine-structure calculations employed here has been previously validated in studies of the lithium atom [18] and the  $\text{C}^+$  ion [19].

## II. METHOD

### A. Nonrelativistic nuclear-mass-dependent Hamiltonian

In the present nonrelativistic variational calculations of the boron atom, it is first necessary to separate out the translational motion of the system as a whole from the internal motion. The corresponding internal Hamiltonian representing the internal motion is obtained by separating out the atom's center-of-mass motion from the nonrelativistic laboratory-frame Hamiltonian. This separation yields an “internal” Hamiltonian, which is used in the present calculations. The separation is rigorous and results in the reduction the  $N$ -particle problem ( $N = 6$  for the boron atom comprising five electrons and a nucleus) to an  $n$ -pseudoparticle problem ( $n = N - 1 = 5$ ) represented by the internal Hamiltonian expressed in terms of the internal Cartesian coordinates,  $\mathbf{r}_i$ 's. In the approach we adopt, these internal coordinates are chosen to be the position vectors of the electrons with respect to the nucleus, which serves as a reference particle. The internal nonrelativistic Hamiltonian has the following form in

atomic units:

$$H_{\text{nr}}^{\text{int}} = -\frac{1}{2} \left( \sum_{i=1}^n \frac{1}{\mu_i} \nabla_{\mathbf{r}_i}^2 + \sum_{i=1}^n \sum_{j \neq i}^n \frac{1}{m_0} \nabla_{\mathbf{r}_i} \cdot \nabla_{\mathbf{r}_j} \right) + \sum_{i=1}^n \frac{q_0 q_i}{r_i} + \sum_{i=1}^n \sum_{j < i}^n \frac{q_i q_j}{r_{ij}}. \quad (1)$$

Here  $q_0 = 5$  is charge of the nucleus,  $q_i = -1$  ( $i = 1, \dots, 5$ ) are the electron charges,  $m_0$  is the nuclear mass ( $m_0 = 18247.468\,631\,92$  for  $^{10}\text{B}$  and  $m_0 = 200\,63.736\,943\,13$  for  $^{11}\text{B}$ ),  $\mu_i = m_0 m_i / (m_0 + m_i)$  is the reduced mass of electron  $i$  ( $m_i = 1$ ,  $i = 1, \dots, 5$ ),  $r_i$  is the distance between the  $i$ th electron and nucleus, and  $r_{ij} = |\mathbf{r}_j - \mathbf{r}_i|$  is the distance between electrons  $i$  and  $j$ . The prime symbol ( $'$ ) stands for the vector/matrix transpose.

The calculations involving the nonrelativistic Hamiltonian  $H_{\text{nr}}^{\text{int}}$  can be carried out for both finite and infinite mass of the B nucleus. They yield the nonrelativistic ground- and excited-state energies ( $E_{\text{nr}}$ ) and the corresponding wave functions. Thus, both the energy and the wave function depend on the mass of the nucleus. In what follows we report both the finite-mass and infinite-mass results.

### B. Basis functions

The all-electron ECG functions employed for expanding the spatial part of the wave functions of  $P$  states in this paper have the following form:

$$\phi_k(\mathbf{r}) = z_{i_k} \exp[-\mathbf{r}' \mathbf{A}_k \mathbf{r}], \quad (2)$$

where  $z_{i_k}$  is the  $z$  coordinate of the  $i_k$ th electron. Subscript  $i_k$ , which is an electron label, can take integer values in the range  $(1, \dots, n)$ . Moreover,  $i_k$  may be treated as an additional integer variational parameter in the calculations. With this, each  $z_{i_k}$  factor can be different in each basis function. The value of  $i_k$  is determined variationally when the gaussian basis function  $\phi_k$  is first added to the basis set. In expression (2),  $\mathbf{r}$  is a  $3n$ -component column vector formed by stacking three-component vectors  $\mathbf{r}_i$  on top of each other and matrix  $\mathbf{A}_k$  is a  $3n \times 3n$  real symmetric matrix of the exponential parameters.  $\mathbf{A}_k$  is constructed as  $\mathbf{A}_k = \mathbf{A}_k \otimes \mathbf{I}$ , where  $\mathbf{A}_k$  is a  $n \times n$  dense real symmetric matrix,  $\mathbf{I}$  is the  $3 \times 3$  identity matrix, and  $\otimes$  denotes the Kronecker product. Such representation of matrix  $\mathbf{A}_k$  ensures that the exponential part of the basis functions is invariant with respect to 3D rotations.

To be used in expanding wave functions of stationary states, each basis function (2) has to be square integrable. This requires that  $\mathbf{A}_k$  matrix is positive definite. To ensure the positive definiteness of  $\mathbf{A}_k$ , it is represented in the Cholesky-factored form as  $\mathbf{A}_k = \mathbf{L}_k \mathbf{L}_k'$ , where  $\mathbf{L}_k$  is a  $n \times n$  lower triangular matrix. In this representation,  $\mathbf{L}_k$  matrix elements can take any real values and the positive definiteness of  $\mathbf{A}_k$  is automatically maintained. This is an important property because it allows varying them without any restrictions in the  $(-\infty$  to  $+\infty)$  range when the variational energy minimization (a numerically very costly procedure) is carried out. For more information on the basis sets see [20,21].

At the lowest-order approximation, the spin-orbit interaction that gives rise to the fine-structure splitting is obtained

as a sum of two terms. In the finite-nuclear-mass (FNM) approach, the first term is an expectation value of the following operator:

$$\begin{aligned}
 H_{\text{SO}} &= H_{\text{SO}_1} + H_{\text{SO}_2} \\
 &= - \sum_{i=1}^n \frac{q_0 q_i}{2m_i} \left( \frac{1}{m_i} + \frac{2}{m_0} \right) \frac{s'_i}{r_i^3} (\mathbf{r}_i \times \mathbf{p}_i) \\
 &\quad - \sum_{\substack{i,j=1 \\ j \neq i}}^n \left\{ \frac{q_0 q_i}{m_0 m_i} \frac{s'_i}{r_i^3} (\mathbf{r}_i \times \mathbf{p}_j) \right. \\
 &\quad \left. + \frac{q_i q_j}{2m_i} \frac{s'_i}{r_{ij}^3} \left[ \mathbf{r}_{ij} \times \left( \frac{1}{m_i} \mathbf{p}_i - \frac{2}{m_j} \mathbf{p}_j \right) \right] \right\} \quad (3)
 \end{aligned}$$

where  $H_{\text{SO}_1}$  and  $H_{\text{SO}_2}$  are the one- and two-electron parts of the  $H_{\text{SO}}$  operator, respectively. They are often referred to as the spin-orbit and spin-other-orbit interactions, respectively. In the lowest order, the fine-structure splitting is calculated as the expectation value of  $H_{\text{SO}}$  using the nonrelativistic wave function obtained in the variational calculation using the internal Hamiltonian (1). Similar to the nonrelativistic Hamiltonian, the Hamiltonian for calculating the spin-orbit interaction also depends on the nuclear mass  $m_0$  [22]. In the limit of an infinite nuclear mass, the Hamiltonian reduces to a sum of the standard spin-orbit and spin-other-orbit interaction operators. Therefore, all recoil corrections to the spin-orbit interaction are automatically included in the calculations. To obtain the leading-order energy correction the expectation value of  $H_{\text{SO}}$  is multiplied by  $\alpha^2$ , where  $\alpha = 1/137.035999084$  is the fine-structure constant. The next-order effect contributing to the fine-structure splitting arises from the anomalous magnetic moment (AMM) of the electron. This term is given by the expectation value of the following Hamiltonian:

$$\begin{aligned}
 H_{\text{AMM}} &= H_{\text{AMM}_1} + H_{\text{AMM}_2} \\
 &= - \sum_{i=1}^n \frac{q_0 q_i}{2m_i^2} \frac{s'_i}{r_i^3} (\mathbf{r}_i \times \mathbf{p}_i) \\
 &\quad - \sum_{\substack{i,j=1 \\ j \neq i}}^n \frac{q_i q_j}{2m_i} \frac{s'_i}{r_{ij}^3} \left[ \mathbf{r}_{ij} \times \left( \frac{1}{m_i} \mathbf{p}_i - \frac{1}{m_j} \mathbf{p}_j \right) \right]. \quad (4)
 \end{aligned}$$

The  $H_{\text{AMM}}$  term is multiplied by  $2\kappa\alpha^2$ , where  $\kappa = 1.15965218128 \times 10^{-3}$  [23] is the electron magnetic moment anomaly. The resulting contribution of this effect is roughly proportional to  $\alpha^3$ . It should be noted that operator  $H_{\text{AMM}}$  is obtained within the infinite-nuclear-mass (INM) approximation and, thus, does not contain any recoil corrections. For more information on the operators see [18,19].

### C. Higher-order corrections

Estimation of the contribution of the higher-order relativistic corrections to the fine-structure splitting of the  $^2P$  states of  $^{\infty}\text{B}$  atom is performed in this paper with the use of the multi-reference methods based on the complete active space (CAS). The orbital Gaussian-type basis set is generated to adequately describe the  $n^2P$  states up to  $n = 11$  considered in the present calculations. The electron

correlation is accounted for within the CASSCF method by the multireference character of the wave function [24–26] and by the second-order perturbation-theory (PT2) correction calculated using the CASPT2 method [27–29]. The spin-orbit interaction is calculated via the restricted active-space state-interaction method (RASSI) [30] using the atomic mean-field integral (AMFI) approximation [31,32]. Within RASSI method the matrix of spin-orbit operator is constructed between all the considered  $n^2P$  states of  $^{\infty}\text{B}$  atom and completed on the main diagonal with the corresponding spin-free energies obtained with CASPT2 method. The eigenvalues of such matrix exhibit the fine-structure splittings including the off-diagonal coupling between different  $n^2P$  states. Inclusion of states of only one  $n^2P$  atomic term within RASSI method provides the corresponding fine-structure splitting without the off-diagonal couplings. The differences in the fine-structure splittings obtained with and without the off-diagonal coupling provides an estimation of the missing  $\alpha^4$  energy terms that are not included in the ECG calculations. All these calculations are performed with the MOLCAS 8.4 computer program [33,34].

The complete contribution at the order of  $\alpha^4$  correction has been established by Puchalski and Pachucki using nonrelativistic QED approach, which has been applied to fine-structure splitting of Li and  $\text{Be}^+$  species [13,35]. A thorough assessment of this correction in more complex systems or excited states is quite intricate. Therefore, some studies have turned to employing the Dirac formula to roughly estimate the  $\alpha^4$  correction for Li [36] and  $\text{O}^{+5}$  [37]. In this paper, the same approach has been adopted to roughly gauge some missing contributions of the order of  $\alpha^4$  and higher. The resulting values have been found to be smaller than the estimated uncertainties of the  $\delta_{\text{offdiag}}$  quantity (see below). For instance, a value of  $1.2 \times 10^{-5} \text{ cm}^{-1}$  has been obtained for the ground state using the Dirac formula, which notably exceeds the values obtained for higher states. Furthermore, the estimated  $\delta_{\text{offdiag}}$  value ( $3.2 \times 10^{-4} \pm 1.6 \times 10^{-4} \text{ cm}^{-1}$ ) are significantly larger than the latter value. For this reason, in this paper, we restrict our analysis by including only the  $\delta_{\text{offdiag}}$  contribution at the  $\alpha^4$  level when computing the fine-structure splittings of  $^2P$  states of boron.

## III. RESULTS

### A. Computational details

Our in-house parallel computer code written in FORTRAN and employing MPI (Message Passing Interface) for the interprocessor communication has been used in the present calculations. The generation of large ECG basis sets together with high accuracy targeted in the calculations requires the use of extended precision (80-bit) arithmetic, which has a hardware implementation in floating-point modules on the x86 architecture. The calculations performed with extended precision are typically slower by a factor of 3–5 compared to more common double-precision calculations. Yet it provides additional 12 bits (or about four decimal figures) of accuracy compared to the standard double precision.

The lowest nine  $^2P$  states of the boron atom have been targeted in this paper. In the first step of the calculations the nonrelativistic wave functions and the corresponding

energies have been determined. The calculations were carried out using the standard variational method and involved the generation of separate sets of the ECG basis functions for each state with progressively larger basis set sizes. The growing of the basis set for a particular state has been performed independently from the other states. The growing process involves adding new functions to the set and variationally optimizing their nonlinear parameters based on a procedure that employs the analytical energy gradient determined with respect to the parameters. More details about the basis set enlargement procedure can be found in our previous papers [17,21]. The generation of the basis sets for each considered state is by far the most time-consuming step of the calculations. It has required over two years of continuous computing using several hundred cores on parallel computer systems equipped with Intel Xeon E5-2695v3 and AMD EPYC 7642 CPUs. In generating the ECG basis sets, we used the internal Hamiltonian that is explicitly dependent on the mass of the nucleus of the  $^{11}\text{B}$  isotope. As the wave function changes very slightly when going from the  $^{11}\text{B}$  to  $^{10}\text{B}$  (or  $^{\infty}\text{B}$ ) isotope the reoptimization of the nonlinear parameters for the other two isotopes is not necessary. The changes in the wave functions are captured with sufficient accuracy by adjusting the linear variational parameters only, which is achieved by solving the generalized eigenvalue problem for a specific isotope using the ECG basis set generated for  $^{11}\text{B}$ .

### B. Nonrelativistic energy

Table I shows the results obtained in the nonrelativistic variational calculations for the lowest nine Rydberg  $^2P$  states of the boron atom using ECG expansions of the wave functions of the considered states and internal Hamiltonian (1). For each  $^2P$  state the nonrelativistic energy is reported for four basis set sizes to demonstrate its numerical convergence with the number of ECGs. Except for the ground state, which has been studied by two other groups using ECG lobe basis functions [41] and ECGs with Cartesian angular factors [13], the excited  $^2P$  states have never been investigated before with highly accurate approaches (e.g., variational method with ECG basis functions). The results obtained in two aforementioned studies are included in the table for comparison. Our previous ECG studies of the spectrum of the boron atom include two reports [16,17]. Very recently, we also performed calculations of the nonrelativistic oscillator strengths for the transitions between low-lying  $^2P$  and  $^2S$  states [42]. In the present study concerning the fine structure of the boron atom, the initial ECG basis sets are taken from our previous study. However, before being used in the present calculations of the fine-structure splittings, the bases were enlarged to 17 000 ECGs. This helped improve the accuracy of the calculated nonrelativistic energies and the convergence of the expectation values of the spin-orbit interaction, as well as make more reliable extrapolations of these quantities in the limit of an infinite basis set.

From the data shown in Table I it is clear that the energies obtained in the present paper are 1 to 4 orders of magnitude more accurate than those reported in previous studies. For instance, the ground state energy of  $-24.653\,867\,537$  hartree was obtained using 8192 ECGs in [13], while our calculation performed with 8000 ECGs yields a lower value

of  $-24.653\,867\,60$  hartree. In addition to the explicitly correlated methods, the boron atom has been studied with other *ab initio* methods, namely the configuration interaction (CI) method [38], the multiconfiguration interaction (MCI) method [40], and the coupled-cluster (CC) method [11]. As it can be deduced from the table where the previous results are compared with the results obtained in the present calculations, the energies obtained using the variational ECG approach show much superior performance.

As the principal quantum number  $n$  increases, the non-relativistic energies in Table I approach the ionization threshold—the ground state of  $\text{B}^+$ , which we also calculated in this paper. Meanwhile, with the increase of  $n$ , the average electron–nucleus distance grows approximately quadratically, ranging from 1.35 bohr for the  $2\ ^2P$  state to 22.27 bohr and 27.94 bohr for the  $9\ ^2P$  and  $10\ ^2P$  states respectively, which confirms their Rydberg nature.

### C. Fine-structure splitting

Table II shows the fine-structure splittings obtained for the considered nine  $^2P$  states of boron in the present paper along with some experimental results from the compilations of [14] and [43] as well as some previous most accurate theoretical results [11,13,40]. The fine-structure splittings are computed as follows:

$$E(n\ ^2P_{3/2}) - E(n\ ^2P_{1/2}) = \underbrace{\alpha^2 C^{\text{SO}} \langle H_{\text{SO}} \rangle}_{\sim \alpha^2} + \underbrace{2\kappa \alpha^2 C^{\text{SO}} \langle H_{\text{AMM}} \rangle}_{\delta_{\text{AMM}}} + \underbrace{\alpha^4 E_{n,\text{SO}}^{\text{offdiag}}}_{\delta_{\text{offdiag}}}, \quad (5)$$

where the expectation values,  $\langle H_{\text{SO}} \rangle$  and  $\langle H_{\text{AMM}} \rangle$ , are calculated between states  $|n\ ^2P, M_S = 1/2, M_L = 1\rangle$ , whose wave functions are obtained for different boron isotopes. The  $C^{\text{SO}} = 3$  factor that appears in Eq. (5) is derived from the recoupling coefficients of the states' angular momenta (for more details see [22]). The last term,  $\delta_{\text{offdiag}}$ , incorporates the off-diagonal corrections to the fine-structure splittings. The  $E_{n,\text{SO}}^{\text{offdiag}}$  is calculated as the difference of the fine-structure splittings calculated with RASSI method (see Sec. II C). However,  $E_{n,\text{SO}}^{\text{offdiag}}$  can be seen in first approximation as the second-order correction to the fine-structure splitting of the state with the principal quantum number  $n$ ,

$$E_{n,\text{SO}}^{(2)} = \sum_{k \neq n} \frac{|\langle \psi_n^{(0)} | H_{\text{SO}} | \psi_k^{(0)} \rangle|^2}{E_n^{(0)} - E_k^{(0)}}, \quad (6)$$

where  $|\psi_n^{(0)}\rangle \equiv |n\ ^2P\rangle$  and  $E_n^{(0)}$  are, respectively, the nonrelativistic wave function and energy of state  $n\ ^2P$ ; here, the summation was limited to the states  $k\ ^2P$  up to  $k = 11$ . It is noted that the contributions from other states of the boron atom within the energy range of the considered  $n\ ^2P$  states vanish either because of the parity or orthogonality of states with different  $J$  quantum numbers. However, there are higher states with  $1s^2 2p^3$  and  $1s^2 2p^2 np$  configurations that may couple via the spin-orbit operator, but their impact, according to our numerical estimates, is expected to be of rather secondary importance.

As it was discussed before, the fine-structure splitting in the ground state of the boron atom was studied before in

TABLE I. Convergence of the nonrelativistic energies of the  $n^2P$  ( $n = 2, \dots, 10$ ) states of  $^{10}\text{B}$ ,  $^{11}\text{B}$ , and  $^{\infty}\text{B}$  atoms with the number of ECG basis functions. All values are in a.u. The present calculations are performed with 12 000–17 000 ECGs and the energies are extrapolated to an infinite basis set limit. For the lowest three states we provide comparison with the best literature values obtained using the configuration interaction (CI), diffusion Monte Carlo (DMC), explicitly correlated Gaussian (ECG), and multiconfiguration interaction (MCI) methods. The numbers in parentheses are estimated numerical uncertainties resulting from the basis truncation.

State	Method	Basis	Reference	$^{10}\text{B}$	$^{11}\text{B}$	$^{\infty}\text{B}$
$2^2P$	ECG	12000	this paper	−24.652 502 43	−24.652 626 07	−24.653 868 27
	ECG	14000	this paper	−24.652 502 57	−24.652 626 21	−24.653 868 42
	ECG	16000	this paper	−24.652 502 69	−24.652 626 33	−24.653 868 54
	ECG	17000	this paper	−24.652 502 70	−24.652 626 34	−24.653 868 55
	ECG	$\infty$	this paper	−24.652 502 84(17)	−24.652 626 48(17)	−24.653 868 69(17)
	CI	$l_{\max} = 20$	[38]			−23.653 837 33
	DMC		[39]			−23.653790(3)
	ECG	8192	[13]			−24.653 867 537
	MCI	$l_{\max} = 6$	[40]			−24.652 032
	ECG lobes		10304	[41]		
ECG lobes	$\infty$	[41]			−24.653 868 90(14)	
$3^2P$	ECG	12000	this paper	−24.430 973 68	−24.431 097 66	−24.432 343 37
	ECG	14000	this paper	−24.430 973 81	−24.431 097 79	−24.432 343 50
	ECG	16000	this paper	−24.430 973 94	−24.431 097 92	−24.432 343 63
	ECG	17000	this paper	−24.430 973 94	−24.431 097 93	−24.432 343 63
	ECG	$\infty$	this paper	−24.430 974 10(18)	−24.431 098 08(18)	−24.432 343 79(18)
	MCI		[40]			−24.389 458
$4^2P$	ECG	12000	this paper	−24.389 169 87	−24.389 293 75	−24.390 538 38
	ECG	14000	this paper	−24.389 170 02	−24.389 293 90	−24.390 538 54
	ECG	16000	this paper	−24.389 170 20	−24.389 294 08	−24.390 538 72
	ECG	17000	this paper	−24.389 170 22	−24.389 294 09	−24.390 538 73
	ECG	$\infty$	this paper	−24.389 170 43(25)	−24.389 294 30(25)	−24.390 538 94(25)
	MCI		[40]			−24.389 458
$5^2P$	ECG	12000	this paper	−24.372 547 12	−24.372 670 95	−24.373 915 06
	ECG	14000	this paper	−24.372 547 34	−24.372 671 17	−24.373 915 28
	ECG	16000	this paper	−24.372 547 55	−24.372 671 37	−24.373 915 49
	ECG	17000	this paper	−24.372 547 61	−24.372 671 43	−24.373 915 55
	ECG	$\infty$	this paper	−24.372 547 81(29)	−24.372 671 64(29)	−24.373 915 75(29)
$6^2P$	ECG	12000	this paper	−24.364 218 78	−24.364 342 57	−24.365 586 40
	ECG	14000	this paper	−24.364 219 21	−24.364 343 00	−24.365 586 83
	ECG	16000	this paper	−24.364 220 00	−24.364 343 79	−24.365 587 62
	ECG	17000	this paper	−24.364 220 03	−24.364 343 82	−24.365 587 65
	ECG	$\infty$	this paper	−24.364 221 0(11)	−24.364 344 8(11)	−24.365 588 6(11)
$7^2P$	ECG	12000	this paper	−24.359 448 1	−24.359 571 9	−24.360 815 5
	ECG	14000	this paper	−24.359 449 3	−24.359 573 1	−24.360 816 7
	ECG	16000	this paper	−24.359 451 7	−24.359 575 5	−24.360 819 1
	ECG	17000	this paper	−24.359 451 8	−24.359 575 6	−24.360 819 3
	ECG	$\infty$	this paper	−24.359 454 6(32)	−24.359 578 3(32)	−24.360 822 0(32)
$8^2P$	ECG	12000	this paper	−24.356 453	−24.356 577	−24.357 821
	ECG	14000	this paper	−24.356 456	−24.356 580	−24.357 823
	ECG	16000	this paper	−24.356 465	−24.356 589	−24.357 832
	ECG	17000	this paper	−24.356 465	−24.356 589	−24.357 833
	ECG	$\infty$	this paper	−24.356 476(12)	−24.356 600(12)	−24.357 843(12)
$9^2P$	ECG	12000	this paper	−24.354 431	−24.354 555	−24.355 798
	ECG	14000	this paper	−24.354 439	−24.354 562	−24.355 806
	ECG	16000	this paper	−24.354 460	−24.354 584	−24.355 827
	ECG	17000	this paper	−24.354 461	−24.354 584	−24.355 828
	ECG	$\infty$	this paper	−24.354 486(29)	−24.354 610(29)	−24.355 854(29)
$10^2P$	ECG	12000	this paper	−24.352 970	−24.353 094	−24.354 337
	ECG	14000	this paper	−24.352 983	−24.353 107	−24.354 351
	ECG	16000	this paper	−24.353 034	−24.353 157	−24.354 401
	ECG	17000	this paper	−24.353 036	−24.353 160	−24.354 403
	ECG	$\infty$	this paper	−24.353 096(68)	−24.353 219(68)	−24.354 463(68)

TABLE I. (*Continued.*)

State	Method	Basis	Reference	$^{10}\text{B}$	$^{11}\text{B}$	$^{\infty}\text{B}$
$\text{B}^+(^1S)$	ECG	5000	this paper	-24.347 517 589 1	-24.347 641 318 4	-24.348 884 476 3
	ECG	$\infty$	this paper	-24.347 517 591 2(25)	-24.347 641 320 5(25)	-24.348 884 478 4(25)

Ref. [13] using ECG basis sets. The value of the fine-structure splitting for the ground state of  $^{11}\text{B}$  obtained in the present paper matches within the uncertainties the values from that earlier calculation [15.288(2)  $\text{cm}^{-1}$ ] and from the NIST ASD database [15.2870(18)  $\text{cm}^{-1}$ ] [14,43]. A fairly good agreement was also obtained using the MCI [40] and MCHF [12] approaches. However, the values obtained in relativistic coupled-cluster calculations [11] deviate significantly from the experiment. It should be noted that, in addition to the ground state, the experimental data on the fine-structure splittings is also available for the  $3^2P$  and  $4^2P$  states of boron. For these states the splitting energies calculated in this paper are in excellent agreement with the experimental values as can be seen in Table II.

In Table II we also include estimated uncertainties of our fine-structure splitting results. The main source of the uncertainty for both lower and higher states can be traced back to two specific factors affecting the accuracy of the calculations, namely the basis set incompleteness and the approximations made in the model used for the fine-structure calculations. Our final values for the splittings in Table II come with two parenthesis. The first one represents the basis truncation error in ECG calculations, while the second one gives an estimated uncertainty arising from approximate calculations of the off-diagonal corrections and neglect of higher-order contributions.

As seen in Table II, the impact of the uncertainty of the off-diagonal corrections on the overall uncertainty of the fine-structure splitting for the ground state is significant ( $\delta_{\text{offdiag}} = 3.2 \times 10^{-4} \text{ cm}^{-1}$ ), but it diminishes with the increase of the principal quantum number. It drops down to below  $10^{-6} \text{ cm}^{-1}$  for the  $n^2P$ ,  $n = 9, 10$  states. Consequently, the effect of the off-diagonal corrections on the uncertainties for the higher states is lower than the accuracy of solving the nonrelativistic problem for these states. Thus, for them the main source of uncertainty is the basis set truncation. For the ground and other low-lying states, however, neglecting the higher-order corrections is likely to be the dominant source of the overall uncertainty. In this paper, we conservatively estimate the combined uncertainty of computing  $\delta_{\text{offdiag}}$  itself and the uncertainty arising from the neglect of higher-order corrections to the fine-structure splittings as 200% of the  $\delta_{\text{offdiag}}$  value.

To the best of our knowledge, the values we report for the fine-structure splittings of the boron atom in this paper are the

most precise to date. The estimated accuracy of our splittings exceeds that of both any previous theoretical calculation and the data available from experiments. We hope that our results could serve as a guide for future experimental measurements, especially for states with larger values of the principal quantum number  $n$ , for which currently there are no data available.

#### IV. SUMMARY

In this paper, high-precision calculations are performed for the lowest nine  $^2P^o$  Rydberg states of the  $^{10}\text{B}$ ,  $^{11}\text{B}$ , and  $^{\infty}\text{B}$  atoms. The nonrelativistic energies and the corresponding wave functions of the considered states are determined in variational calculations where the BO approximation is not assumed (i.e., the nucleus is treated on the same footing as the electrons). The wave functions of the considered states are expanded in terms of all-particle explicitly correlated Gaussian basis functions and up to 17 000 functions are used for each state. The nonlinear exponential parameters of the Gaussians are extensively optimized using a procedure based on the Rayleigh–Ritz variational principle. The procedure involves the use of the analytical energy gradient determined with respect to the parameters. Very accurate nonrelativistic energies and the corresponding wave functions are generated. Next, the wave functions are used to compute the fine-structure splittings of the considered states of  $^{10}\text{B}$ ,  $^{11}\text{B}$ , and  $^{\infty}\text{B}$ . The calculated values are in very good agreement with the available experimental data for the ground  $2^2P$ , and excited  $3^2P$  and  $4^2P$  states. They also reveal that more accurate measurements are needed to provide verification of the results calculated in this paper. For the most of the considered Rydberg states, these results are the first high-precision values calculated to date.

#### ACKNOWLEDGMENTS

This paper has been supported by the National Science Foundation (Grant No. 1856702) and Nazarbayev University (Faculty Development Grant No. 021220FD3651). Authors acknowledge the use of computational resources at the University of Arizona High Performance Computing, Nazarbayev University Research Computing, and Institute of Theoretical Physics and Astrophysics, University of Gdansk, Poland.

TABLE II. Fine-structure splittings of states  $n^2P$  ( $n = 2, \dots, 10$ ) of the boron atom in  $\text{cm}^{-1}$ . The leading-order ( $\sim\alpha^2$ ) contribution is calculated as the expectation value in state  $|n^2P, M_S = \frac{1}{2}, M_L = 1\rangle$  of the  $\langle H_{\text{SO}} \rangle$  Hamiltonian shown in Eq. (5). The  $\delta_{\text{AMM}}$  is the  $2\kappa\alpha^2$  ( $\approx \alpha^3/\pi$ ) contribution representing the anomalous magnetic moment term calculated as the expectation value  $\langle H_{\text{AMM}} \rangle$  of the Hamiltonian shown in Eq. (4). The  $\delta_{\text{offdiag}}$  term is the off-diagonal correction calculated with multireference methods using one-electron Gaussian orbitals (see Sec. II C). The numbers in the first parentheses are numerical uncertainties resulting from the finite size of the ECG basis set used. The numbers in the second parentheses are estimated uncertainties arising from neglecting higher-order corrections. The best literature values for the fine-structure splittings are included for comparison, with some abbreviations borrowed from the previous table. In addition, CC and MCHF stand for the relativistic coupled-cluster method and multiconfiguration Hartree–Fock method, respectively.

State	Method	Basis	Reference	Contribution	$^{10}\text{B}$	$^{11}\text{B}$	$^{\infty}\text{B}$
$2^2P$	ECG	17000	this paper	$\alpha^2$	15.245 899	15.245 995	15.246 957
	ECG	$\infty$	this paper	$\alpha^2$	15.245 913(20)	15.246 007(20)	15.246 972(20)
	ECG	17000	this paper	$\alpha^2 + \delta_{\text{AMM}}$	15.287 040	15.287 136	15.288 098
	ECG	$\infty$	this paper	$\alpha^2 + \delta_{\text{AMM}}$	15.287 054(20)	15.287 148(20)	15.288 112(20)
	ECG	$\infty$	this paper	$\alpha^2 + \delta_{\text{AMM}} + \delta_{\text{offdiag}}$	15.287 374(20)(640)	15.287 468(20)(640)	15.288 432(20)(640)
	MCI		[40]	$\alpha^2 + \delta_{\text{AMM}}$			15.523
	CC		[11]	$\alpha^2$			19.75
	MCHF		[12]	$\alpha^2$			15.39
	ECG		[13]	$\alpha^2 + \delta_{\text{AMM}}$			15.287 8(20)
	Experiment		[14,43]		15.287 0(40)	15.287 0(18)	
$3^2P$	ECG	17000	this paper	$\alpha^2$	1.778 127	1.778 132	1.778 179
	ECG	$\infty$	this paper	$\alpha^2$	1.778 146(45)	1.778 152(45)	1.778 224(45)
	ECG	17000	this paper	$\alpha^2 + \delta_{\text{AMM}}$	1.782 894	1.782 899	1.782 947
	ECG	$\infty$	this paper	$\alpha^2 + \delta_{\text{AMM}}$	1.782 913(45)	1.782 919(45)	1.782 992(45)
	ECG	$\infty$	this paper	$\alpha^2 + \delta_{\text{AMM}} + \delta_{\text{offdiag}}$	1.782 813(45)(210)	1.782 819(45)(210)	1.782 892(45)(210)
	MCI		[40]	$\alpha^2 + \delta_{\text{AMM}}$			1.7103
	CC		[11]	$\alpha^2$			0.80
		Experiment		[14,43]		1.782 0(57)	1.783 0(50)
$4^2P$	ECG	17000	this paper	$\alpha^2$	0.634 552	0.634 553	0.634 564
	ECG	$\infty$	this paper	$\alpha^2$	0.634 556(15)	0.634 557(15)	0.634 571(15)
	ECG	17000	this paper	$\alpha^2 + \delta_{\text{AMM}}$	0.636 258	0.636 259	0.636 270
	ECG	$\infty$	this paper	$\alpha^2 + \delta_{\text{AMM}}$	0.636 262(15)	0.636 263(15)	0.636 277(15)
	ECG	$\infty$	this paper	$\alpha^2 + \delta_{\text{AMM}} + \delta_{\text{offdiag}}$	0.636 187(15)(150)	0.636 188(15)(150)	0.636 202(15)(150)
	MCI		[40]	$\alpha^2 + \delta_{\text{AMM}}$			0.803 7
	Experiment		[14,43]		0.63(14)	0.635(30)	
$5^2P$	ECG	17000	this paper	$\alpha^2$	0.300 483	0.300 483	0.300 482
	ECG	$\infty$	this paper	$\alpha^2$	0.300 486(17)	0.300 489(17)	0.300 488(17)
	ECG	17000	this paper	$\alpha^2 + \delta_{\text{AMM}}$	0.301 292	0.301 292	0.301 292
	ECG	$\infty$	this paper	$\alpha^2 + \delta_{\text{AMM}}$	0.301 296(17)	0.301 299(17)	0.301 297(17)
	ECG	$\infty$	this paper	$\alpha^2 + \delta_{\text{AMM}} + \delta_{\text{offdiag}}$	0.301 227(17)(140)	0.301 230(17)(140)	0.301 228(17)(140)
$6^2P$	ECG	17000	this paper	$\alpha^2$	0.165 938	0.165 937	0.165 924
	ECG	$\infty$	this paper	$\alpha^2$	0.165 939(25)	0.165 938(25)	0.165 924(25)
	ECG	17000	this paper	$\alpha^2 + \delta_{\text{AMM}}$	0.166 386	0.166 384	0.166 371
	ECG	$\infty$	this paper	$\alpha^2 + \delta_{\text{AMM}}$	0.166 387(25)	0.166 385(25)	0.166 372(25)
	ECG	$\infty$	this paper	$\alpha^2 + \delta_{\text{AMM}} + \delta_{\text{offdiag}}$	0.166 327(25)(120)	0.166 325(25)(120)	0.166 312(25)(120)
$7^2P$	ECG	17000	this paper	$\alpha^2$	0.101 209	0.101 206	0.101 182
	ECG	$\infty$	this paper	$\alpha^2$	0.101 171(39)	0.101 169(39)	0.101 135(39)
	ECG	17000	this paper	$\alpha^2 + \delta_{\text{AMM}}$	0.101 482	0.101 480	0.101 456
	ECG	$\infty$	this paper	$\alpha^2 + \delta_{\text{AMM}}$	0.101 444(39)	0.101 442(39)	0.101 408(39)
	ECG	$\infty$	this paper	$\alpha^2 + \delta_{\text{AMM}} + \delta_{\text{offdiag}}$	0.101 429(39)(30)	0.101 427(39)(30)	0.101 393(39)(30)
$8^2P$	ECG	17000	this paper	$\alpha^2$	0.066 25	0.066 24	0.066 22
	ECG	$\infty$	this paper	$\alpha^2$	0.066 12(11)	0.066 12(11)	0.066 10(11)
	ECG	17000	this paper	$\alpha^2 + \delta_{\text{AMM}}$	0.066 43	0.066 42	0.066 40
	ECG	$\infty$	this paper	$\alpha^2 + \delta_{\text{AMM}}$	0.066 30(11)	0.066 30(11)	0.066 28(11)
	ECG	$\infty$	this paper	$\alpha^2 + \delta_{\text{AMM}} + \delta_{\text{offdiag}}$	0.066 30(11)(0)	0.066 30(11)(0)	0.066 28(11)(0)
$9^2P$	ECG	17000	this paper	$\alpha^2$	0.045 88	0.045 88	0.045 85
	ECG	$\infty$	this paper	$\alpha^2$	0.045 64(26)	0.045 64(26)	0.045 61(26)
	ECG	17000	this paper	$\alpha^2 + \delta_{\text{AMM}}$	0.046 01	0.046 00	0.045 98
	ECG	$\infty$	this paper	$\alpha^2 + \delta_{\text{AMM}}$	0.045 76(26)	0.045 76(26)	0.045 74(26)
	ECG	$\infty$	this paper	$\alpha^2 + \delta_{\text{AMM}} + \delta_{\text{offdiag}}$	0.045 76(26)(0)	0.045 76(26)(0)	0.045 74(26)(0)

TABLE II. (*Continued.*)

State	Method	Basis	Reference	Contribution	$^{10}\text{B}$	$^{11}\text{B}$	$^{\infty}\text{B}$
$10\ ^2P$	ECG	17000	this paper	$\alpha^2$	0.033 27	0.033 27	0.033 24
	ECG	$\infty$	this paper	$\alpha^2$	0.033 04(32)	0.033 04(32)	0.033 01(32)
	ECG	17000	this paper	$\alpha^2 + \delta_{\text{AMM}}$	0.033 36	0.033 36	0.033 33
	ECG	$\infty$	this paper	$\alpha^2 + \delta_{\text{AMM}}$	0.033 13(32)	0.033 13(32)	0.033 10(32)
	ECG	$\infty$	this paper	$\alpha^2 + \delta_{\text{AMM}} + \delta_{\text{offdiag}}$	0.033 13(32)(0)	0.033 13(32)(0)	0.033 10(32)(0)

- [1] N. Grevesse, M. Asplund, and A. Sauval, The solar chemical composition, *Space Sci. Rev.* **130**, 105 (2007).
- [2] A. M. Brooks, K. A. Venn, D. L. Lambert, M. Lemke, K. Cunha, and V. V. Smith, Boron in the small Magellanic cloud: A novel test of light-element production, *Astrophys. J.* **573**, 584 (2002).
- [3] D. S. Dearborn, D. N. Schramm, G. Steigman, and J. Truran, The shocking development of lithium (and boron) in supernovae, *Astrophys. J.* **347**, 455 (1989).
- [4] G. Valle, F. Ferrini, D. Galli, and S. N. Shore, Evolution of Li, Be, and B in the galaxy, *Astrophys. J.* **566**, 252 (2002).
- [5] J. N. Bahcall and R. A. Wolf, Fine-structure transitions, *Astrophys. J.* **152**, 701 (1968).
- [6] A. K. Pradhan and S. N. Nahar, *Atomic Astrophysics and Spectroscopy* (Cambridge University Press, Cambridge, 2011).
- [7] C. R. Proffitt, D. J. Lennon, N. Langer, and I. Brott, Stellar boron abundances near the main-sequence turnoff of the open cluster NGC 3293 and implications for the efficiency of rotationally driven mixing in stellar envelopes, *Astrophys. J.* **824**, 3 (2016).
- [8] S. Randich and L. Magrini, Light elements in the universe, *Front. Astron. Space Sci.* **8**, 616201 (2021).
- [9] S. Mrozowski, Über den Isotopenverschiebungseffekt im Spektrum des Bors, *Z. Phys.* **112**, 223 (1939).
- [10] E. W. Burke, Isotope shift in the first three spectra of boron, *Phys. Rev.* **99**, 1839 (1955).
- [11] H. Gharibnejad and A. Derevianko, Coupled-cluster calculations of properties of the boron atom as a monovalent system, *Phys. Rev. A* **86**, 022505 (2012).
- [12] C. F. Fischer and G. Tachiev, Breit–Pauli energy levels, lifetimes, and transition probabilities for the beryllium-like to neon-like sequences, *At. Data Nucl. Data Tables* **87**, 1 (2004).
- [13] M. Puchalski, J. Komasa, and K. Pachucki, Explicitly correlated wave function for a boron atom, *Phys. Rev. A* **92**, 062501 (2015).
- [14] A. E. Kramida, Yu. Ralchenko, J. Reader, and NIST ASD Team, NIST Atomic Spectra Database (ver. 5.11) [Online] (2023), available at <http://physics.nist.gov/asd>.
- [15] S. Bubin and L. Adamowicz, Correlated-Gaussian calculations of the ground and low-lying excited states of the boron atom, *Phys. Rev. A* **83**, 022505 (2011).
- [16] S. Bubin and L. Adamowicz, Lowest  $^2S$  electronic excitations of the boron atom, *Phys. Rev. Lett.* **118**, 043001 (2017).
- [17] I. Hornyák, S. Nasiri, S. Bubin, and L. Adamowicz,  $^2S$  Rydberg spectrum of the boron atom, *Phys. Rev. A* **104**, 032809 (2021).
- [18] S. Nasiri, J. Liu, S. Bubin, M. Stanke, A. Kędziorowski, and L. Adamowicz, Oscillator strengths and interstate transition energies involving  $^2S$  and  $^2P$  states of the Li atom, *At. Data Nucl. Data Tables* **149**, 101559 (2023).
- [19] M. Stanke, A. Kędziorowski, S. Nasiri, L. Adamowicz, and S. Bubin, Fine structure of the  $^2P$  energy levels of singly ionized carbon (C II), *Phys. Rev. A* **108**, 012812 (2023).
- [20] S. Bubin and L. Adamowicz, Energy and energy gradient matrix elements with  $N$ -particle explicitly correlated complex Gaussian basis functions with  $L = 1$ , *J. Chem. Phys.* **128**, 114107 (2008).
- [21] S. Bubin, M. Pavanello, W.-C. Tung, K. L. Sharkey, and L. Adamowicz, Born–Oppenheimer and non-Born–Oppenheimer, atomic and molecular calculations with explicitly correlated Gaussians, *Chem. Rev.* **113**, 36 (2013).
- [22] A. Kędziorowski, M. Stanke, and L. Adamowicz, Atomic fine-structure calculations performed with a finite-nuclear-mass approach and with all-electron explicitly correlated Gaussian functions, *Chem. Phys. Lett.* **751**, 137476 (2020).
- [23] E. Tiesinga, P. J. Mohr, D. B. Newell, and B. N. Taylor, CODATA recommended values of the fundamental physical constants: 2018, *Rev. Mod. Phys.* **93**, 025010 (2021).
- [24] B. O. Roos, P. R. Taylor, and P. E. Sigbahn, A complete active space SCF method (CASSCF) using a density matrix formulated super-CI approach, *Chem. Phys.* **48**, 157 (1980).
- [25] B. O. Roos, The complete active space SCF method in a Fock-matrix-based super-CI formulation, *Int. J. Quant. Chem.* **18**, 175 (1980).
- [26] B. O. Roos, The Complete active space self-consistent field method and its applications in electronic structure calculations, *Adv. Chem. Phys.* **69**, 399 (1987).
- [27] K. Andersson, P. Å. Malmqvist, B. O. Roos, A. J. Sadlej, and K. Wolinski, Second-order perturbation theory with a CASSCF reference function, *J. Phys. Chem.* **94**, 5483 (1990).
- [28] K. Andersson, P.-Å. Malmqvist, and B. O. Roos, Second-order perturbation theory with a complete active space self-consistent field reference function, *J. Chem. Phys.* **96**, 1218 (1992).
- [29] J. Finley, P.-Å. Malmqvist, B. O. Roos, and L. Serrano-Andrés, The multi-state CASPT2 method, *Chem. Phys. Lett.* **288**, 299 (1998).
- [30] P.-Å. Malmqvist, B. O. Roos, and B. Schimmelpfennig, The restricted active space (RAS) state interaction approach



- with spin-orbit coupling, *Chem. Phys. Lett.* **357**, 230 (2002).
- [31] B. A. Heß, C. M. Marian, U. Wahlgren, and O. Gropen, A mean-field spin-orbit method applicable to correlated wavefunctions, *Chem. Phys. Lett.* **251**, 365 (1996).
- [32] B. Schimmelpfennig, L. Maron, U. Wahlgren, C. Teichteil, H. Fagerli, and O. Gropen, On the combination of ECP-based CI calculations with all-electron spin-orbit mean-field integrals, *Chem. Phys. Lett.* **286**, 267 (1998).
- [33] F. Aquilante, J. Autschbach, A. Baiardi, S. Battaglia, V. A. Borin, L. F. Chibotaru, I. Conti, L. De Vico, M. Delcey, I. Fdez. Galván *et al.*, Modern quantum chemistry with [Open]Molcas, *J. Chem. Phys.* **152**, 214117 (2020).
- [34] F. Aquilante, J. Autschbach, R. K. Carlson, L. F. Chibotaru, M. G. Delcey, L. De Vico, I. Fdez. Galván, N. Ferré, L. M. Frutos, L. Gagliardi *et al.*, MOLCAS 8: New capabilities for multiconfigurational quantum chemical calculations across the periodic table, *J. Comput. Chem.* **37**, 506 (2016).
- [35] M. Puchalski and K. Pachucki, Quantum electrodynamics corrections to the  $2P$  fine splitting in Li, *Phys. Rev. Lett.* **113**, 073004 (2014).
- [36] L. M. Wang, Y. P. Zhang, D. Sun, and Z.-C. Yan, Nonrelativistic energies and fine-structure splittings for the Rydberg  $P$  states of lithium, *Phys. Rev. A* **102**, 052815 (2020).
- [37] L. M. Wang and Z.-C. Yan, Transition frequencies between the  $2S$  and  $2P$  states of the lithiumlike ion  $O^{5+}$ , *Phys. Rev. A* **100**, 032505 (2019).
- [38] C. X. Almora-Díaz and C. F. Bunge, Nonrelativistic CI calculations for  $B^+$ , B, and  $B^-$  ground states, *Int. J. Quantum Chem.* **110**, 2982 (2010).
- [39] P. Seth, P. L. Ríos, and R. J. Needs, Quantum Monte Carlo study of the first-row atoms and ions, *J. Chem. Phys.* **134**, 084105 (2011).
- [40] C. Chen, Energies, expectation values, fine structures and hyperfine structures of the ground state and excited states for boron, *Eur. Phys. J. D* **69**, 128 (2015).
- [41] K. Strasburger, Energy difference between the lowest doublet and quartet states of the boron atom, *Phys. Rev. A* **102**, 052806 (2020).
- [42] S. Nasiri, S. Bubin, and L. Adamowicz, Oscillator strengths for  $^2P - ^2S$  transitions in neutral boron, *Phys. Rev. A* **109**, 042813 (2024).
- [43] A. E. Kramida and A. N. Ryabtsev, A critical compilation of energy levels and spectral lines of neutral boron, *Phys. Scr.* **76**, 544 (2007).